High Chern number quantum anomalous Hall effect tunable by stacking order in van der Waals topological insulators

Wenxuan Zhu, Cheng Song,* Hua Bai, Liyang Liao, and Feng Pan†
Key Laboratory of Advanced Materials, School of Materials Science and Engineering, Beijing Innovation Center for Future Chips, Tsinghua University, Beijing 100084, China

(Received 4 December 2021; accepted 8 February 2022; published 14 April 2022)

The discovery of van der Waals (vdW) $MnBi_2Te_4$ provides a platform for investigating the quantum anomalous Hall effect (QAHE), which is a candidate for quantum computation without dissipation. However, because of the topological requirement, the High Chern number QAHE with extended dissipation-free channels is hard to achieve in atomically thin samples, which can take full advantage of two-dimensional (2D) materials. In this work, by first-principles calculations, the variable stacking order (inherent to vdW materials) was proposed as a means of regulating the Chern number of the QAHE in $MnBi_2Te_4$ (MBT). The interlayer stacking order in the 2D limit dominates the orbital hybridization, resulting in a tunable topological property. Furthermore, the High Chern number QAHE with $C = N$ was achieved in ultrathin MBT ($2N$ septuple layers) with alternate stacking orders, which have different topological states. This scenario was extended to the vdW heterostructure of MBT-family materials for achieving a stable, zero-field, High Chern number QAHE. Our work reveals stacking tunable topological properties in vdW magnetic topological insulators and provides an effective means of regulating the QAHE.

DOI: 10.1103/PhysRevB.105.155122

Topologically protected quantum states, robust against local perturbations, are unique features in topological materials [1,2]. Especially in the context of introducing ferromagnetism into the topologically nontrivial band structure ($Z_2 \neq 0$) in topological insulators (TIs), the magnetic order breaks the time-reversal symmetry, and a chiral edge mode between the opened Dirac point at the surface states is evident [1,3,4]. The chiral edge mode gives rise to the QAHE; its dissipation-free edge channel is promising for future low-power quantum computations [5,6]. The Chern number (C) determines the number of the chiral edge channels, and characterizes the topological invariance of the band structure [7,8]. The QAHE with a high Chern number ($C > 1$), which provides more dissipation-free channels, can reduce the contact resistance in devices and facilitate quantum computations [9,10]. The QAHE with $C = 1$ has been widely observed in several magnetic TIs, such as Cr- and V-doped $(Bi, Sb)_2Te_3$ [11–13], and magnetic insulator/TI heterostructures by the proximity effect [14,15]. The recent discovery of intrinsic van der Waals (vdW) topological magnetic TI $MnBi_2Te_4$ (MBT) provides an ideal platform for achieving the QAHE [16–20]. Nevertheless, because of the topological requirement, massive stacked bulk materials with a large thickness are generally necessary to increase the Chern number to higher quantized values ($C > 1$), such as bulk MBT with ten septuple layers (SLs) (>13 nm) [21]; so doing decreases the advantage of vdW two-dimensional (2D) materials. Another possibility for achieving a high Chern number is constructing heterostructures with multiperiod topological and conventional insulator layers, in which the large-thickness requirement remains because of the spacer layer of a conventional insulator [22,23]; researchers require an efficient method for regulating the QAHE in the 2D limit.

Based on flexible construction, which is a characteristic of 2D materials [24], research on the QAHE has considerably advanced. CrI_3/MBT [25], MBT/VBi_2Te_4 (VBT), and MBT/$EuBi_2Te_4$ (EBT) heterostructures [26,27] are predicted to transform the interlayer antiferromagnetic coupling of MBT into ferromagnetic coupling, which can stabilize the magnetic configurations and surface states; in so doing, the requirement of an external magnetic field for the QAHE will be eliminated. The combination of MBT and Bi_2Te_3 layers can also increase the critical temperature of the QAHE to several kelvin [28,29]. Another more important inherent feature of 2D materials, the variable interlayer stacking order, provides a new possibility for regulating intrinsic properties. A variable stacking order has been achieved through molecular-beam epitaxy, which can be used to tune the interlayer magnetic coupling in various 2D magnetic materials [30–34] and determine the interlayer ferroelectric polarization in hexagonal boron nitride [35]. Moreover, the stacking orders are also predicted and observed to regulate various topological states in nonmagnetic low-dimensional vdW topological materials [36–38], such as ternary transition-metal chalcogenides. Therefore, the variable stacking order is a promising procedure within the 2D limit for regulating the QAHE in vdW magnetic TIs.

In this work, by first-principles calculations based on density-functional theory [39–43], we achieved the QAHE with a tunable high Chern number by regulating the stacking order in an MBT multilayer. By regulating the interlayer stacking order, both topologically trivial and nontrivial states

*songcheng@mail.tsinghua.edu.cn
†panf@mail.tsinghua.edu.cn

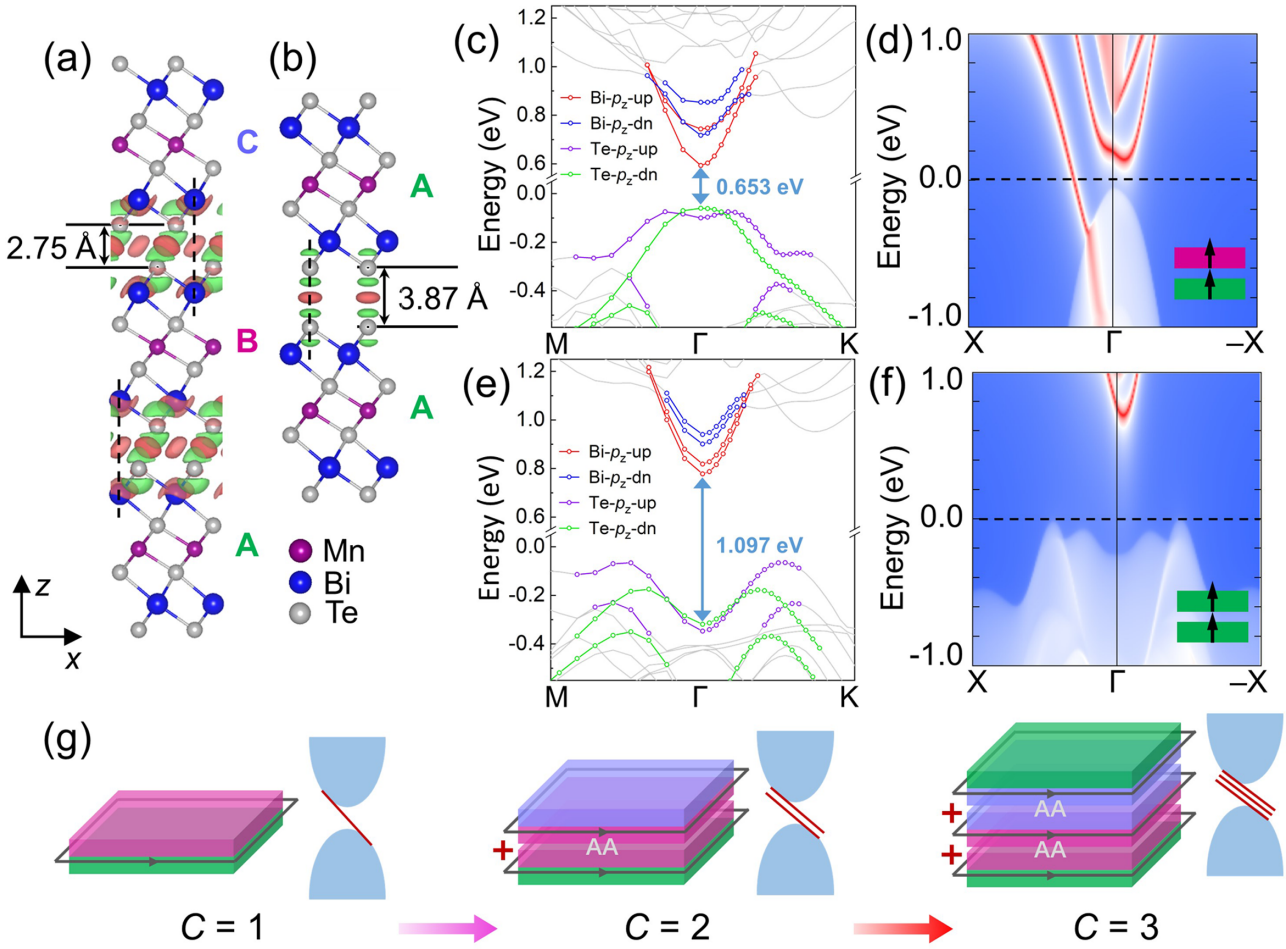

FIG. 1. (a,b) Structures and interlayer differential charge densities of A-B-C (a) and A-A (b) stacked $MnBi_2Te_4$ (MBT). (c–f) Band structures without spin-orbit coupling and left edge states of an MBT bilayer in A-B stacking order (c,d), and A-A stacking order (e,f). (g) Schematic of the High Chern number quantum anomalous Hall effect in an MBT multilayer with alternate stacking orders. The black arrows indicate the chiral edge channels of the MBT layers.

in MBT were obtained in a bilayer MBT, which was determined by the hybridization of the interlayer Te p orbitals. The QAHE with $C = N$ was achieved in $2N$ -SL MBT with alternate stacking orders, which exhibit topologically trivial and nontrivial properties. The nontrivial layer, which can tune the Chern number, was reduced to an interface. Furthermore, a robust High Chern number QAHE with zero field was also predicted in MBT/VBT with a similar arrangement of stacking orders.

Figure 1(a) shows a vdW magnetic TI MBT, composed of layered Te-Bi-Te-Mn-Te-Bi-Te SLs with a stacking order of A-B-C [16]. In the pristine stacking order A-B-C, each SL shifts $1/3$ in-plane distance between two Mn atoms along the x direction and the interlayer Bi atoms from two SLs are aligned in the z direction. Another high symmetric stacking order, which has also been observed and proposed in many other 2D materials [30,31,33,34,44], is A-A [Fig. 1(b)]. The Mn atoms of two adjacent SLs are aligned in the z direction. In the A-B-C and A-A stacking orders, the stacking of the interlayer Te atoms is also distinct, which can lead to different topological properties. In A-B-C, the interlayer Te atoms are staggered along the z direction with a smaller interlayer distance of 2.75 Å and a large interlayer charge redistribution was achieved in the vdW gap between layers as illustrated by the differential charge density (DCD) in Fig. 1(a). The large charge redistribution resided not only between the interlayer Te atoms but also around the Bi atoms away from the interlayer vdW gap, leading to the strong interlayer coupling.

The significant interlayer DCD indicates the strong hybridization between the valance electron orbitals of interlayer Te atoms, i.e., $5p$ orbitals, and we describe such p-p interaction as "quasibonding." The interlayer quasibonding of Te-p_z orbitals would consequently lift its antibondinglike state toward the Fermi level in the valance bands [37]. Therefore, the strength of the interlayer quasibonding is pertinent to increasing the top of the valance bands occupied by the Te-p_z orbitals at the Γ point in k space. In the situation of AB stacking with large interlayer hybridization and strong quasi-bonding, a direct band gap was formed with a small gap energy without consideration of spin-orbit coupling (SOC) [Fig. 1(c)]. By introducing SOC, the direct band gap with small gap energy led to the appearance of topologically nontrivial band structure with band inversion between Bi-p_z and Te-p_z orbitals at the Γ point [25,45]. The QAHE with $C = 1$ was achieved in an A-B stacked MBT bilayer when an external field was applied to align the antiferromagnetically coupled moments and break

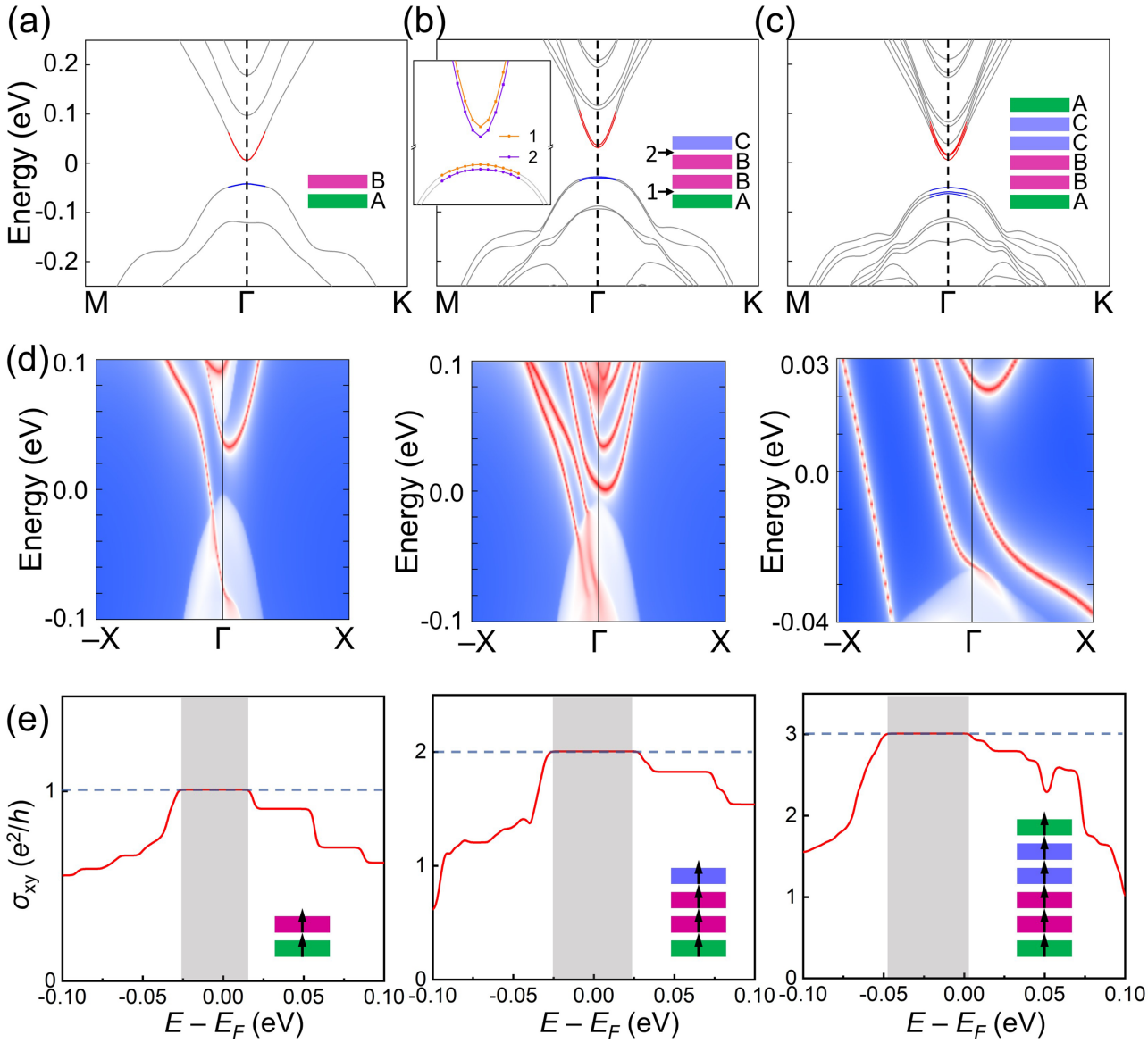

FIG. 2. (a–c) Band structure with spin-orbit coupling of a high Chern quantum anomalous Hall effect (QAHE) multilayer. The insets show schematics of the stacking order. An additional inset in (b) indicates the band projection from the two A-B stacked bilayers. The inversion between the Bi-p_z and Te-p_z orbitals at the Γ point is highlighted in blue and red, respectively. (d,e) Left edge state (d) and anomalous Hall conductance (e) of a High Chern number QAHE multilayer. The insets in (e) show the magnetic configurations.

the time-reversal symmetry, indicated by the chiral edge state [Fig. 1(d)]. In contrast, the interlayer distance in the A-A stacking order was much larger and a less-redistributed charge was mainly present between the interlayer Te atoms indicating a much weaker interlayer hybridization and quasibonding between interlayer Te-p orbitals compared to AB stacking [Fig. 1(d)]. Due to the weaker interlayer quasibonding and atomic force, the total energy of AA stacking was 71 meV/f.u. higher than the ground state of MBT with AB stacking. The small energy difference makes it possible for AA stacking to also exist in practical situations. Most importantly, the weak interlayer hybridization in the A-A stacking made the Te-p_z orbitals which occupy the top of the valance bands at the Γ point possess lower-energy states. This led to an indirect band gap with a much larger gap energy, as highlighted in the band structure without SOC [Fig. 1(e)]. Therefore, a topologically trivial property without an edge state was obtained by introducing SOC [Fig. 1(f)]. In addition to the effect of the interlayer distance, the orientation of the interlayer Bi-Te bonding also influenced the interlayer orbital hybridization when taking another stacking A-C into consideration [43].

In an N-layer ferromagnetic Weyl semimetal (WSM), the ideal anomalous Hall conductance (AHC) is given by $\sigma_{xy} = N|\tilde{k}_W|e^2/h$, in which $|\tilde{k}_W|$ denotes the ratio of Γ-W (Weyl point) to Γ-Z along the Γ-Z direction in k space [21,26]. Because of the topological requirement, σ_{xy} is quantized in vdW WSM. Therefore, the AHC is $\sigma_{xy} = ([N|\tilde{k}_W|] + 1)e^2/h$ and an increase of the Chern number by 1 requires an increase of the layer number $\Delta N = 1/|\tilde{k}_W|$, resulting in the large thickness required for achieving a high Chern QAHE

[21,26]. In addition to increasing in thickness, another possibility for achieving a high Chern number is sandwiching the magnetic WSM with a conventional insulator. Because of the topologically trivial band structure in conventional insulator layers, the AHC of this heterostructure changes to $\sigma_{xy} = \sum_{i=1}^{n}([N_i|\tilde{k}_W|_i] + 1)e^2/h$, in which n denotes the number of topologically nontrivial layers separated by topologically trivial layers. In this scenario, accumulation of one cycle of a magnetic WSM/conventional insulator [22] (or a WSM/magnetic insulator [24]) increases the Chern number by 1.

As demonstrated in previous paragraphs, distinct topological states in MBT are also readily obtained by adjusting the interlayer stacking order, which is a straightforward means of constructing a high Chern QAHE system. As an interface, the interlayer stacking order enables regulation of the Chern number in the 2D limit, reducing the thickness to an atomically thin scale compared with the previous utilization of a conventional insulator as a spacer layer between the WSM layers. Based on this guidance, the interlayer stacking orders of an MBT multilayer was designed, based on the A-A and A-B-C stacking orders; the magnetic moment of each SL was aligned in the same direction along the z axis to break the time-reversal symmetry. Figure 1(g) shows a schematic of our design. The MBT bilayer in A-B stacking with one chiral edge state ($C = 1$) is the basic building block of a high Chern MBT multilayer. By combing two A-B stacked MBT bilayers with an A-A stacking order, a topologically trivial interface was created between two magnetic WSM layers, which resulted in a doubling of the chiral edge states ($C = 2$). On this foundation, further accumulating one A-B stacked unit with an interlayer A-A stacking order achieved a tripling of the edge modes.

The band structure with SOC and topological properties of MBT multilayers was investigated; the Supplemental Material shows the corresponding atomic structures [43]. Figure 2(a) shows the topologically nontrivial band structure of an A-B stacked MBT bilayer. With both SOC and strong interlayer hybridization indicated in Fig. 1(a), a pair of band inversions between the p_z orbitals of interlayer Bi and Te atoms was formed at the Γ point in k space. When two A-B bilayers were spaced by an A-A stacked interface [Fig. 2(b), inset], the bands at the top of the valance bands and the bands at the bottom of the conduction bands split. Consequently, the number of the inversed bands doubled [Fig. 2(b)]. The effect of the dipole resulting from the broken symmetry of the structure was also excluded through the comparison with the band structure after the dipole correction [43]. Generally, in a pristine MBT multilayer with consistent A-B-C stacking, every Bi-Te/Te-Bi at the interlayer interface is topologically nontrivial and coupled through strong interlayer orbital hybridizations, resulting in an overlap of their energy bands [43]. In contrast, the weak interlayer coupling of A-A stacking splits the bands around the Fermi level; they are contributed by the two separated A-B stacked bilayers [Fig. 2(b)]. It is important that the interlayer hybridization shown in Fig. 1(b) ensures magnetic coupling between two A-B units separated by an A-A stacked interface. The comparatively weak but still evident interlayer coupling in A-A stacking prevents the degradation of bands from two A-B units, which will happen when two A-B units are completely decoupled. Therefore, two pairs of band inversions composed of Bi-p_z and Te-p_z orbitals become evident, reflecting the feature of $C = 2$. Furthermore, a nontrivial band structure with triple band inversions was obtained in three A-B bilayer units separated by a topologically trivial A-A interface [Fig. 2(c)], which indicates the QAHE with $C = 3$.

Figures 2(d) and 2(e) show the edge state and AHC (σ_{xy}) of the designed MBT multilayers, which provide direct evidence for the high Chern number QAHE. In Fig. 2(d), with accumulation of each MBT bilayer in A-B stacking separated by the interface of the A-A stacking, the number of the chiral edge states of the surface state increases by 1. The increased chiral edge state leads to enhancement of the quantized σ_{xy} [Fig. 2(e)], which further demonstrates the high Chern number QAHE.

Although the A-A stacking changes the topological properties of MBT, the interlayer antiferromagnetic coupling of MBT remains unchanged, with an energy of 0.3 meV/u.c. (unit cell), which is lower than that of ferromagnetic coupling [43], as the result of the half-occupied d orbitals of Mn^{2+} [26,27]. Considering that the designed MBT multilayers remain antiferromagnetically coupled, an external magnetic field remains essential for achieving a robust, high Chern number QAHE, which is unfavorable for practical applications. Theoretical predictions indicate that by combining MBT with other vdW magnetic TIs from the same family,

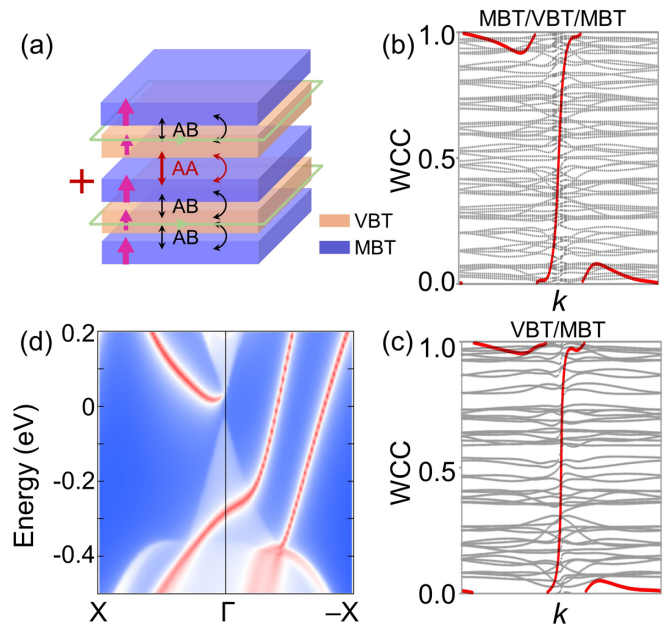

FIG. 3. (a) Schematic and magnetic ground state of five septuple layer (5 SL) $MnBi_2Te_4$ (MBT)/MBT/VBi_2Te_4 (VBT) heterostructures with alternate stacking orders. The pink arrow indicates the magnetic moment of each layer. The green arrows indicate the chiral edge channels of the MBT/VBT layers. (b,c) Wannier charge center loops of A-B-C stacked MBT/VBT/MBT (b) and A-B stacked VBT/MBT (c). Red curves represent the evolution of the sum of Wannier charge center of all occupied states. (d) Right edge state of a five SL MBT/VBT heterostructure with $C = 2$.

the magnetic ions of which have empty orbitals [such as VBT (V^{2+}) and EBT (Eu^{2+})], researchers can create interlayer ferromagnetic coupling through interlayer exchange interactions. Ferromagnetically coupled MBT/VBT(EBT) heterostructures retain their topologically nontrivial property and achieve a robust, zero-field QAHE in both an odd and even number of layers. Therefore, alternate stacking orders were extended to MBT/VBT heterostructures for achieving a robust, high Chern number QAHE with zero field.

First, the A-A stacked MBT/VBT bilayer exhibited interlayer ferromagnetic coupling with a total energy of 0.2 meV/u.c. (lower than that of antiferromagnetic coupling [43]); which was the same as that of A-B stacking. Considering that the quite small band gap of the MBT/VBT bilayer at the Γ point corresponds to challenges in the context of achieving multiple edge states [27], A-B-C stacked MBT/VBT/MBT three-SLs were combined with an A-B stacked VBT/MBT bilayer through an A-A stacking order, which concomitantly ensured a large band gap and a minimal layer number. The five-SL–MBT/VBT heterostructure exhibited the ground state of interlayer ferromagnetic coupling with an out of plane magnetic easy axis in each layer [43]; Fig. 3(a) shows a schematic, and the Supplemental Material shows its atomic structure [43]. First, MBT/VBT/MBT and VBT/MBT were both topologically nontrivial with $C = 1$ without an external magnetic field, indicated by the Wannier charge center loops in k space in Figs. 3(b) and 3(c), respectively. By combining these two parts with $C = 1$ through an A-A stacking order, a zero-field magnetic TI with $C = 2$ was obtained. The double gapless chiral edge states [Fig. 3(d)] indicate dual channels for dissipation-free quantum computation at zero magnetic field.

In conclusion, utilizing the advantage of the variable stacking order that is unique in vdW materials, we regulated the Chern number of the QAHE in an MBT multilayer. The number of chiral edge states was increased by accumulating topologically nontrivial layers, which were separated by trivial stacked interfaces, providing more channels for QAHE-based quantum computations. Our design will facilitate reduction of the large cost of the thickness of an interface upon increasing the Chern number (compared with previous scenarios), such as by constructing heterostructures with multiperiod topological and conventional insulators. Methods for preparing a vdW single layer and heterostructures by precise control (such as by mechanical exfoliation and transfer, and molecular-beam epitaxy) will facilitate development of the proposed structure. Our work provides a means of achieving a high Chern number QAHE system and will facilitate corresponding regulation through the stacking order in 2D materials.

This work was supported by the National Key R&D Program of China (Grant No. 2021YFB3601301), the National Natural Science Foundation of China (Grant No. 51871130), and the Natural Science Foundation of Beijing, China (Grant No. JQ20010).

[1] M. Z. Hasan and C. L. Kane, Colloquium: Topological insulators, Rev. Mod. Phys. **82**, 3045 (2010).
[2] X. L. Qi and S. C. Zhang, Topological insulators and superconductors, Rev. Mod. Phys. **83**, 1057 (2011).
[3] L. Fu and C. L. Kane, Topological insulators with inversion symmetry, Phys. Rev. B **76**, 045302 (2007).
[4] Y. L. Chen, J. H. Chu, J. G. Analytis, Z. K. Liu, K. Igarashi, H. H. Kuo, X. L. Qi, S. K. Mo, R. G. Moore, D. H. Lu *et al.*, Massive Dirac fermion on the surface of a magnetically doped topological insulator, Science **329**, 659 (2010).
[5] C. Nayak, S. H. Simon, A. Stern, M. Freedman, and S. Das Sarma, Non-Abelian anyons and topological quantum computation, Rev. Mod. Phys. **80**, 1083 (2008).
[6] H. Weng, R. Yu, X. Hu, X. Dai, and Z. Fang, Quantum anomalous Hall effect and related topological electronic states, Adv. Phys. **64**, 227 (2015).
[7] J. E. Avron, R. Seiler, and B. Simon, Homotopy and Quantization in Condensed Matter Physics, Phys. Rev. Lett. **51**, 51 (1983).
[8] M. den Nijs, Quantized Hall Conductance in a Two-Dimensional Periodic Potential, Phys. Rev. Lett. **49**, 405 (1984).
[9] J. Wang, B. Lian, H. Zhang, Y. Xu, and S. C. Zhang, Quantum Anomalous Hall Effect with Higher Plateaus, Phys. Rev. Lett. **111**, 136801 (2013).
[10] C. Z. Chang, W. Zhao, D. Y. Kim, P. Wei, J. K. Jain, C. Liu, M. H. W. Chan, and J. S. Moodera, Zero-Field Dissipationless Chiral Edge Transport and the Nature of Dissipation in the Quantum Anomalous Hall State, Phys. Rev. Lett. **115**, 057206 (2015).
[11] C. Z. Chang, J. Zhang, X. Feng, J. Shen, Z. Zhang, M. Guo, K. Li, Y. Ou, P. Wei, L. L. Wang *et al.*, Experimental observation of the quantum anomalous Hall effect in a magnetic topological insulator, Science **340**, 167 (2013).
[12] J. G. Checkelsky, R. Yoshimi, A. Tsukazaki, K. S. Takahashi, Y. Kozuka, J. Falson, M. Kawasaki, and Y. Tokura, Trajectory of the anomalous Hall effect towards the quantized state in a ferromagnetic topological insulator, Nat. Phys. **10**, 731 (2014).
[13] K. M. Fijalkowski, N. Liu, P. Mandal, S. Schreyeck, K. Brunner, C. Gould, and L. W. Molenkamp, Quantum anomalous Hall edge channels survive up to the Curie temperature, Nat. Commun. **12**, 5599 (2021).
[14] Y. Hou, J. Kim, and R. Wu, Magnetizing topological surface states of Bi_2Se_3 with a CrI_3 monolayer, Sci. Adv. **5**, eaaw1874 (2019).
[15] J. Zhang, B. Zhao, T. Zhou, Y. Xue, C. Ma, and Z. Yang, Strong magnetization and Chern insulators in compressed graphene/CrI_3 van der Waals heterostructures, Phys. Rev. B **97**, 085401 (2018).
[16] J. Li, Y. Li, S. Du, Z. Wang, B. L. Gu, S. C. Zhang, K. He, W. Duan, and Y. Xu, Intrinsic magnetic topological insulators in van der Waals layered $MnBi_2Te_4$-family materials, Sci. Adv. **5**, eaaw5685 (2019).
[17] Y. Deng, Y. Yu, M. Z. Shi, Z. Guo, Z. Xu, J. Wang, X. H. Chen, and Y. Zhang, Quantum anomalous Hall effect in intrinsic magnetic topological insulator $MnBi_2Te_4$, Science **367**, 895 (2020).

[18] C. Liu, Y. Wang, H. Li, Y. Wu, Y. Li, J. Li, K. He, Y. Xu, J. Zhang, and Y. Wang, Robust axion insulator and Chern insulator phases in a two-dimensional antiferromagnetic topological insulator, Nat. Mater. **19**, 522 (2020).

[19] C. Liu, Y. Wang, M. Yang, J. Mao, H. Li, Y. Li, J. Li, H. Zhu, J. Wang, L. Li *et al.*, Magnetic-field-induced robust zero Hall plateau state in $MnBi_2Te_4$ Chern insulator, Nat. Commun. **12**, 4647 (2021).

[20] D. Ovchinnikov, X. Huang, Z. Lin, Z. Fei, J. Cai, T. Song, M. He, Q. Jiang, C. Wang, H. Li *et al.*, Intertwined topological and magnetic orders in atomically thin Chern insulator $MnBi_2Te_4$, Nano Lett. **21**, 2544 (2021).

[21] J. Ge, Y. Liu, J. Li, H. Li, T. Luo, Y. Wu, Y. Xu, and J. Wang, High-Chern-number and high-temperature quantum Hall effect without Landau levels, Natl. Sci. Rev. **7**, 1280 (2020).

[22] G. Jiang, Y. Feng, W. Wu, S. Li, Y. Bai, Y. Li, Q. Zhang, L. Gu, X. Feng, D. Zhang *et al.*, Quantum anomalous Hall multilayers grown by molecular beam epitaxy, Chin. Phys. Lett. **35**, 076802 (2018).

[23] Y. F. Zhao, R. Zhang, R. Mei, L. J. Zhou, H. Yi, Y. Q. Zhang, J. Yu, R. Xiao, K. Wang, N. Samarth *et al.*, Tuning the Chern number in quantum anomalous Hall insulators, Nature (London) **588**, 419 (2020).

[24] C. Gong and X. Zhang, Two-dimensional magnetic crystals and emergent heterostructure devices, Science **363**, eaav4450 (2019).

[25] H. Fu, C. X. Liu, and B. Yan, Exchange bias and quantum anomalous Hall effect in the $MnBi_2Te_4/CrI_3$ heterostructure, Sci. Adv. **6**, eaaz0948 (2020).

[26] Z. Li, J. Li, K. He, X. Wan, W. Duan, and Y. Xu, Tunable interlayer magnetism and band topology in van der Waals heterostructures of $MnBi_2Te_4$-family materials, Phys. Rev. B **102**, 081107(R) (2020).

[27] W. Zhu, C. Song, L. Liao, Z. Zhou, H. Bai, Y. Zhou, and F. Pan, Quantum anomalous Hall insulator state in ferromagnetically ordered $MnBi_2Te_4/VBi_2Te_4$ heterostructures, Phys. Rev. B **102**, 085111 (2020).

[28] S. Qi, R. Gao, M. Chang, Y. Han, and Z. Qiao, Pursuing the high-temperature quantum anomalous Hall effect in $MnBi_2Te_4/Sb_2Te_3$ heterostructures, Phys. Rev. B **101**, 014423 (2020).

[29] H. Deng, Z. Chen, A. Wołoś, M. Konczykowski, K. Sobczak, J. Sitnicka, I. V. Fedorchenko, J. Borysiuk, T. Heider, Ł. Pluciński *et al.*, High-temperature quantum anomalous Hall regime in a $MnBi_2Te_4/Bi_2Te_3$ superlattice, Nat. Phys. **17**, 36 (2021).

[30] T. Song, Z. Fei, M. Yankowitz, Z. Lin, Q. Jiang, K. Hwangbo, Q. Zhang, B. Sun, T. Taniguchi, K. Watanabe *et al.*, Switching 2D magnetic states via pressure tuning of layer stacking, Nat. Mater. **18**, 1298 (2019).

[31] T. Li, S. Jiang, N. Sivadas, Z. Wang, Y. Xu, D. Weber, J. E. Goldberger, K. Watanabe, T. Taniguchi, C. J. Fennie *et al.*, Pressure-controlled interlayer magnetism in atomically thin CrI_3, Nat. Mater. **18**, 1303 (2019).

[32] W. Chen, Z. Sun, Z. Wang, L. Gu, X. Xu, S. Wu, and C. Gao, Direct observation of van der Waals stacking–dependent interlayer magnetism, Science **366**, 983 (2019).

[33] N. Sivadas, S. Okamoto, X. Xu, C. J. Fennie, and D. Xiao, Stacking-dependent magnetism in bilayer CrI_3, Nano Lett. **18**, 7658 (2018).

[34] W. Zhu, C. Song, Y. Zhou, Q. Wang, H. Bai, and F. Pan, Insight into interlayer magnetic coupling in 1T-type transition metal dichalcogenides based on the stacking of nonmagnetic atoms, Phys. Rev. B **103**, 224404 (2021).

[35] M. Vizner Stern, Y. Waschitz, W. Cao, I. Nevo, K. Watanabe, T. Taniguchi, E. Sela, M. Urbakh, O. Hod, and M. Ben Shalom, Interfacial ferroelectricity by van der Waals sliding, Science **372**, 1462 (2021).

[36] J. Liu, H. Wang, C. Fang, L. Fu, and X. Qian, Van der Waals stacking-induced topological phase transition in layered ternary transition metal chalcogenides, Nano Lett. **17**, 467 (2020).

[37] R. Peng, Y. Ma, H. Wang, B. Huang, and Y. Dai, Stacking-dependent topological phase in bilayer MBi_2Te_4 (M = Ge, Sn, Pb), Phys. Rev. B **101**, 115427 (2020).

[38] R. Noguchi, M. Kobayashi, Z. Jiang, K. Kuroda, T. Takahashi, Z. Xu, D. Lee, M. Hirayama, M. Ochi, T. Shirasawa *et al.*, Evidence for a higher-order topological insulator in a three-dimensional material built from van Der Waals stacking of bismuth-halide chains, Nat. Mater. **20**, 473 (2021).

[39] G. Kresse and J. Furthmuller, Efficient iterative schemes for *ab initio* total-energy calculations using a plane-wave basis set, Phys. Rev. B **54**, 11169 (1996).

[40] J. P. Perdew, K. Burke, and M. Ernzerhof, Generalized Gradient Approximation Made Simple, Phys. Rev. Lett. **77**, 3865 (1996).

[41] S. Grimme, J. Antony, S. Ehrlich, and H. Krieg, A consistent and accurate *ab initio* parametrization of density functional dispersion correction (DFT-D) for the 94 elements H-Pu, J. Chem. Phys. **132**, 154104 (2010).

[42] Q. S. Wu, S. N. Zhang, H. F. Song, M. Troyer, and A. A. Soluyanov, WANNIERTOOLS: An open-source software package for novel topological materials, Comput. Phys. Commun. **224**, 405 (2018).

[43] See Supplemental Material at http://link.aps.org/supplemental/10.1103/PhysRevB.105.155122 for calculation methods, discussion on the interlayer orbital hybridization, total energy with different magnetic configurations without SOC, total energy with different magnetic anisotropy, band structure after the dipole correction, band structure of 4-SL MBT, and atomic structures of heterostructures.

[44] C. Wang, X. Zhou, L. Zhou, Y. Pan, Z. Y. Lu, X. Wan, X. Wang, and W. Ji, Bethe-Slater-curve-like behavior and interlayer spin-exchange coupling mechanisms in two-dimensional magnetic bilayers, Phys. Rev. B **102**, 020402(R) (2020).

[45] J. Li, C. Wang, Z. Zhang, B. L. Gu, W. Duan, and Y. Xu, Magnetically Controllable Topological Quantum Phase Transitions in the Antiferromagnetic Topological insulator $MnBi_2Te_4$, Phys. Rev. B **100**, 121103(R) (2019).